Volume 3, Issue 5 (Electronics, Magnetics and Photonics) 2018 , pp. 255-260

Smooth TiO_2 Thin Films Grown by Aqueous Spray Deposition for Long-Wave Infrared Applications

Journal:	*MRS Advances*
Manuscript ID	MRSF17-2789318.R2
Manuscript Type:	Symposium EM10
Date Submitted by the Author:	n/a
Complete List of Authors:	Alhasan, Sarmad; University of Central Florida, Electrical and Computer Engineering Calhoun, Seth; University of Central Florida, Physics Abouelkhair, Hussain; University of Central Florida, Physics Lowry, Vanessa; University of Central Florida, Physics Peale, Robert; University of Central Florida, Physics Rezadad, Imen; Nanospective Smith, Evan; US Air Force Research Laboratory, Sensors Directorate Cleary, Justin; Air Force Research Laboratory, Sensors Directorate Oladeji, Isaiah; SISOM THIN FILMS LLC,
Keywords:	spray deposition, Ir, thin film

Volume 3, Issue 5 (Electronics, Magnetics and Photonics) 2018 , pp. 255-260

Smooth TiO_2 Thin Films Grown by Aqueous Spray Deposition for Long-Wave Infrared Applications

Sarmad Fawzi Hamza Alhasan,[1,2] Seth R. Calhoun,[3] Hussain Abouelkhair,[3] Vanessa C. Lowry,[3] Robert E. Peale,[3] Imen Rezadad,[4] Evan M. Smith[5,6] Justin W. Cleary,[6] Isaiah O. Oladeji[7]

[1]*Electrical and Computer Engineering, University of Central Florida, Orlando, FL 32816-2362, USA*

[2]*Laser and Optoelectronics Engineering, University of Technology, Baghdad IRAQ.*

[3]*Physics, University of Central Florida, Orlando FL 32816-2385 USA*

[4]*NanoSpective Inc, 12565 Research Parkway, Ste. 390, Orlando FL 32826 USA*

[5]*KBRWyle, Beavercreek OH 45431 USA.*

[6]*Air Force Research Laboratory, Sensors Directorate, Wright-Patterson AFB OH 45433, USA*

[7]*SISOM Thin Films LLC, 1209 West Gore Street, Orlando, FL 32805, USA. info@sisomtf.com*

ABSTRACT

Self-assembled TiO_2 films deposited by aqueous-spray deposition were investigated to evaluate morphology, crystalline phase, and infrared optical constants. The Anatase nano-crystalline film had ~10 nm characteristic surface roughness sparsely punctuated by defects of not more than 200 nm amplitude. The film is highly transparent throughout the visible to wavelengths of 12 μm. The indirect band gap was determined to be 3.2 eV. Important for long-wave infrared applications is that dispersion in this region is weak compared with the more commonly used dielectric SiO_2 for planar structures. An example application to a metal-insulator-metal resonant absorber is presented. The low-cost, large-area, atmospheric-pressure, chemical spray deposition method allows conformal fabrication on flexible substrates for long-wave infrared photonics.

INTRODUCTION

Titanium dioxide is a very well-studied material with wide ranging applications, as discussed in [1]. TiO_2 films have been deposited by a wide variety of methods, representatively summarized in [1]. This paper considers TiO_2 as a potentially

Volume 3, Issue 5 (Electronics, Magnetics and Photonics) 2018 , pp. 255-260

useful material for long-wave infrared applications motivated by the relatively low dispersion for TiO_2 in the 8 to 12 μm wavelength range, in comparison to commonly-used SiO_2. This work presents a potentially advantageous aqueous deposition method that provides smooth conformal coatings. We designate the film considered here as "smooth SPEED" TiO_2 to distinguish it from a highly structured film grown by a different SPEED recipe reported earlier [1], which was designated "Ropy SPEED" according to its observed morphology.

The complex refractive index spectra have been reported out to far infrared wavelengths (125 μm) for TiO_2 thin films prepared by vacuum-based physical deposition [2,3]. Our atmospheric-pressure aqueous inhomogeneous-chemical-reaction method has unique potential for low cost, large area, perfectly conformal [1, 4] roll-to-roll manufacturing. Physical and optical properties of such films are reported here with particular emphasis on application to infrared photonics, such as metal-insulator-metal plasmonic resonant absorbers [5] and planer waveguides [6].

METHODS

Streaming Process for Electrodeless Electrochemical Deposition (SPEED) grows films by heterogeneous reaction, with little wasteful homogeneous reaction, in contrast to chemical bath deposition. Hydrophilic substrates bind hydroxyl ion (OH^-) nucleation sites with density > 10^{12} cm^{-3}. Substrate heating provides reaction activation energy. Precursors comprised titanium chloride in organic solvents and 20%-by-volume deionized water, which sources OH- and oxygen. Ethanol, isopropanol, and methyl propanol are complexing agents for Ti ions. Films were grown on bare or aluminum-coated silicate glass. Both surfaces are hydrophilic and readily anchor OH^- ions, which attract positively charged complexes to initiate electrochemical reaction without external field or electrodes. The heterogeneous chemical reactions are

$$[Sub](OH)^- + [TiL_n]^{p+(4+)} \rightarrow [Sub]Ti(OH)^{3+} + (L_n)^p\uparrow \quad (1)$$

$$[Sub]Ti(OH)^{3+} + 3OH^- \rightarrow [Sub]TiO_2 + 2H_2O\uparrow \quad (2)$$

where L is an organic ligand, [Sub] the substrate, p the ligand charge, and n the number of ligands coordinated with Ti. Substrate temperature must exceed the reaction activation energy and suffice to eliminate by-products by decomposition and evaporation (up arrows). Site regeneration follows

$$[Sub]TiO_2 + OH^- \rightarrow [Sub]TiO_2(OH)^- . \quad (3)$$

The freshly attached OH^- initiates the next cycle. Growth competition leads to nanoparticle morphology.

Asymmetric out-of-plane X-ray Diffraction (PANalytical Empyrean, XRD) used CuKα radiation (λ= 0.154059 nm) at incidence angle 1 deg. XRD data were compared with reference spectra for Anatase, Rutile, and Brookite (International Centre for Diffraction Data, PDF2 Release 2015). Scanning electron microscopy (Zeiss ULTRA-55) imaged surface. Cut and polished cross-sections (Allied Multiprep Polishing System-12 and 10:1 Buffered Oxide Etch) were imaged using scanning ion beam microscopy (Zeiss Cross Beam FIB). Samples for SEM imaging were sputter coated with 2 nm Iridium (Gatan Precision Etching Coating System).

Atomic Force Microscopy (Digital Instruments 5000U, AFM, with Gwyddion software) gave surface roughness map. Transmittance spectra (Cary 500i) determined

Volume 3, Issue 5 (Electronics, Magnetics and Photonics) 2018 , pp. 255-260

band gap. Optical constants were determined by spectroscopic ellipsometry using a J. A. Woollam IR-VASE.

RESULTS

Figure 1 (left) presents XRD results, which show that smooth SPEED TiO_2 on Al-coated glass is Anatase phase. Growth of TiO_2 on a conducting substrate was motivated by the LWIR applications presented below.) Aluminum peaks are also observed.

Figure 1 (right) presents SEM images of the top surface of the film. The surface is mostly smooth and featureless, except for small scattered blisters of ~ 1 μm lateral dimensions. In the smooth regions, the microstructure has ~20 nm length scale. These films are suitable for long-wave infrared (LWIR) applications, because those wavelengths (~10 μm) are much larger than the surface defects. Blisters may form from a combination compressive stress and poor adhesion, noting that the thermal expansion coefficients of aluminum and anatase are significantly different, or these surface defects may be non-volatized by-products.

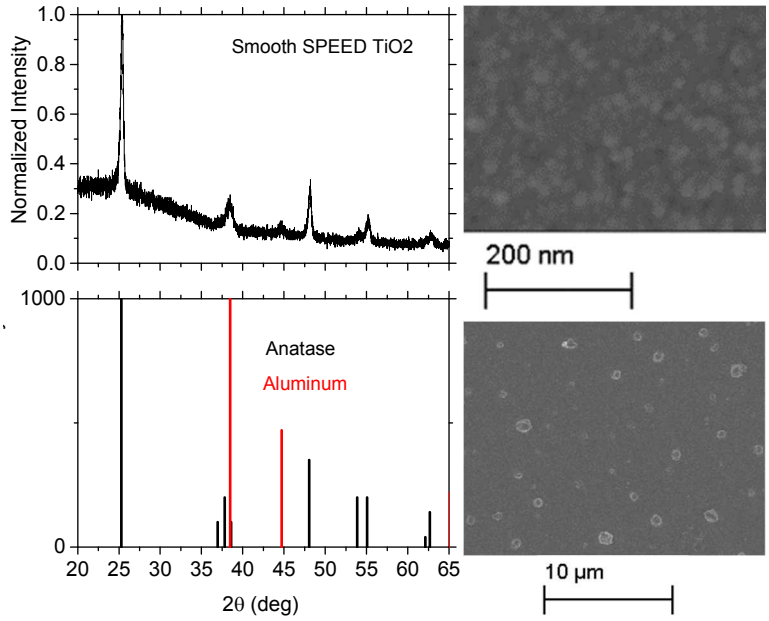

Figure 1. (left) XRD of TiO_2 film and reference. (right) SEM images of smooth-SPEED TiO_2 film surface.

Figure 2 (left) presents a cross section showing substrate, Al & TiO_2 layers, and 200 nm scale bar. The TiO_2 film is ~ 130 nm thick. Figure 2 (right) shows surface morphology comprising sparse and isolated narrow peaks of ~200 nm amplitude and ~ 1 μm wide base on a smooth background of ~10 nm roughness, which is consistent with the SEM image in Figure 1.

Volume 3, Issue 5 (Electronics, Magnetics and Photonics) 2018 , pp. 255-260

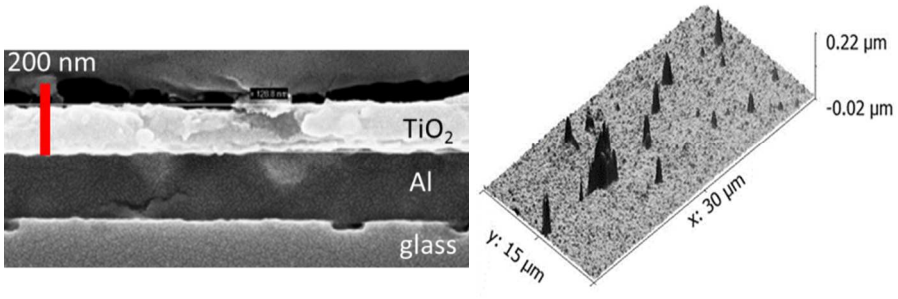

Figure 2. (left) SEM cross-sectional images of Smooth SPEED TiO_2 film. (right) AFM image of Smooth SPEED TiO_2.

Figure 3 (left) presents a UV-visible transmission spectrum for a film on glass, using bare glass reference. The refractive index of Anatase at 2.5 eV is ~3 for unpolarized light and random crystallite orientation [7], giving 25% Fresnel reflectance at 500 nm wavelength. The 80% peak transmittance somewhat exceeds expectations, which may be a due to interference within the film, since the optical thickness n*d ~ 390 nm exceeds half the 500 nm wavelength. This is supported by the observation of one full Fabry-Perot oscillation for a 210 nm thick evaporated TiO_2 film. For the thinner smooth-SPEED film, Fabry-Perot fringes should be separated by 1.5 eV, and a weak bump appears 1.2 eV below the 3 eV peak. The smaller than expected period may be due to truncation by fundamental absorption above 3 eV.

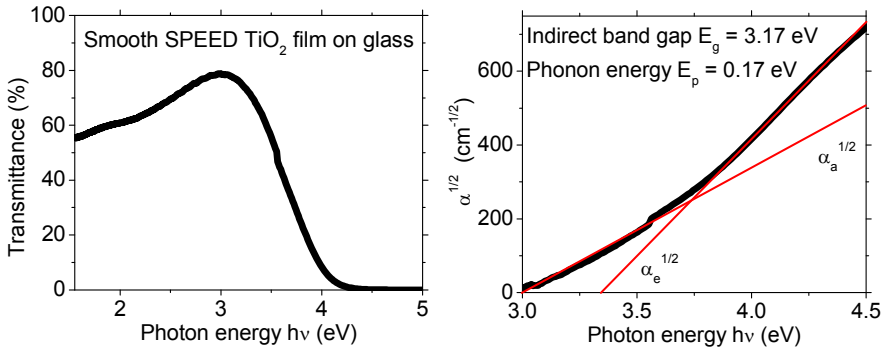

Figure 3. (left) Transmission spectrum. (right) Determination of E_g.

Figure 3 (right) presents determination of the indirect gap of anatase [7] E_g. Absorption coefficient α was calculated according to Beer's law $\ln(1/T)/d$ from film thickness d and the transmittance spectrum T, which was normalized to remove Fresnel reflectance. The absorption edge depends on absorption and emission of phonons with energy E_p, according to [8]

$$\alpha_e + \alpha_a = C_e(T)\,(h\nu - E_g - E_p)^2 + C_a(T)\,(h\nu - E_g + E_p)^2 \quad , \qquad (4)$$

where the coefficients depend on temperature-dependent phonon statistics. A plot of the square root of equation 4 gives two straight segments, whose extensions to $\alpha = 0$ define $E_g \pm E_p$. The determined values are given in the Figure. If $\sqrt{\alpha}h\nu$ is plotted instead [9], somewhat larger values $E_g = 3.21$ eV and $E_p = 0.21$ eV are found. E_g is usually reported

Volume 3, Issue 5 (Electronics, Magnetics and Photonics) 2018 , pp. 255-260

to be in the range 3.08-3.35 eV [7, 10-14]. The E_p value is about twice the onset of optical phonon absorption, shown below.

At high energies, the absorption coefficient goes as $\sqrt{(h\nu - E_g')}$, where E_g' is the direct gap. We find E_g' to be about 4.2 eV by extrapolating a plot of α^2 (or $(\alpha h\nu)^2$) to zero absorption. This value is higher than the expected value 3.8 eV [7]. However, the spectral region that follows the square root dependence is narrow with very low transmittance, so that our value of E_g' has high uncertainty.

Figure 4 (left) compares infrared spectra of refractive index n and extinction coefficient κ for smooth SPEED TiO_2 to those for evaporated SiO_2. The TiO_2 spectra compare well with previous reports for differently prepared films [2,3]. SiO_2 has a strong and sharp extinction peak near 9 μm wavelength, but the TiO_2 extinction is comparatively weak out to at least 11 μm wavelength. Thus, TiO_2 would be better than SiO_2 as an index contrast material for LWIR photonic planer waveguides due to its comparatively low loss [6]. Moreover, TiO_2 lacks the derivative-like dispersion feature observed for n of SiO_2, which allows TiO_2-based metal-insulator-metal (MIM) absorbers to have single resonances for spectral sensing applications as opposed to the complicated spectra observed for SiO_2-based devices [15]. Figure 4 (right) demonstrates the difference for SiO_2- and SPEED-TiO_2-based MIM structures with (top-square, dielectric thicknesses) = (3.1 μm, 1.3 μm) and (1.31 μm, 0.104 μm), respectively.

The onset of extinction beyond 12 μm wavelength suggests optical phonon energies less than 0.1 eV. This is agreement with optical phonon frequencies determined from far-infrared reflectivity [16]. Thus, the determined E_p value (Figure 3) is surprisingly large, unless the absorption is a two phonon process.

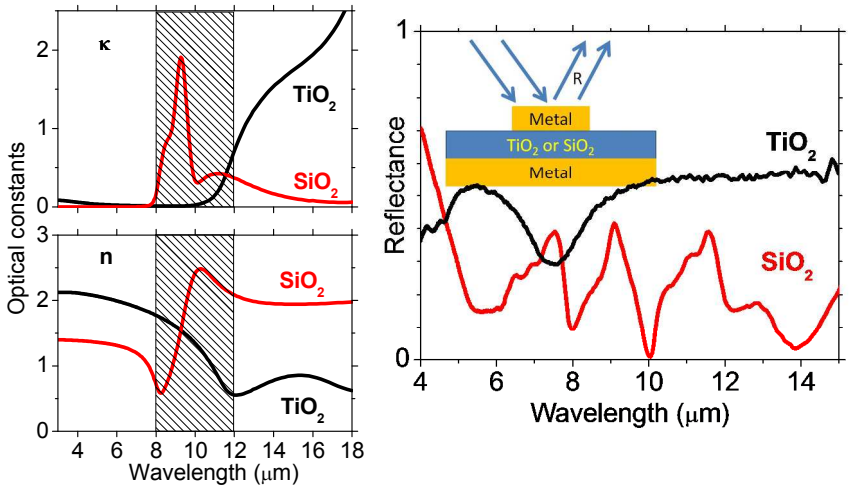

Figure 4. (left) Infrared complex index spectra for smooth SPEED TiO_2 and evaporated SiO_2 films. The shaded region indicates LWIR wavelengths. (right) Reflectance spectra of SiO_2 and SPEED TiO_2-based MIM devices.

DISCUSSEION AND CONCLUSIONS

Alternative aqueous spray methods of TiO_2 film deposition include liquid tetraisopropyl titanate (TPT) and water separately picked up by inert carrier gas, mixed, then sprayed on heated substrate (100-400 C) [17]. Deposition rate was only 0.1-1 nm/sec. Only optical characterization without microstructural information were

Volume 3, Issue 5 (Electronics, Magnetics and Photonics) 2018 , pp. 255-260

presented. In contrast, SPEED TiO_2 films grew at 100-1000 higher rates by directly spraying an aqueous solution containing titanium ions and ligands onto substrates at 300-400 C.

Spray pyrolysis [18] of organo-metallic compounds to grow TiO_2 requires sufficient heat to break (lyse) precursor molecules, whereas SPEED proceeds via heterogeneous chemical reaction, heat being used mainly to evaporate reaction by-products.

Spray coating of TiO_2 film can be done at ambient conditions using a suspension of precrystallized nano-particles [19]. Resulting smooth films up to 30 nm thick suffice for electron-transport in solar cells, but this is too thin for infrared applications. Such films are less adhesive than SPEED films, which are chemically-bound to the surface, in our experience.

In conclusion, optical and morphological properties of Smooth Anatase TiO_2 film grown by aqueous spray deposition were presented. Defects are much smaller than long-wave infrared wavelengths and should not contribute significantly to electrodynamic losses. Low dispersion in the long-wave infrared is attractive for resonant absorbers in applications that require low loss and spectral selectivity.

ACKNOWLEDGMENTS

The work of SFHA was supported in part by the Higher Committee for Education Development in Iraq (HCED), Prime Minister Office, IRAQ, Baghdad. http://hcediraq.org/.

REFERENCES

1. S. Alhasan, F. Khalilzadeh-Rezaie, R.E. Peale, and I. Oladeji, *MRS Advances,* **1**, 3169 (2016).
2. T. Siefke, S. Kroker, K. Pfeiffer, O. Puffky, K. Dietrich, D. Franta, I. Ohlídal, A. Szeghalmi, E.-B. Kley, and A. Tünnermann, *Adv. Opt. Mater.* **4**, 1780 (2016).
3. J. Kischkat, S. Peters, B. Gruska, M. Semtsiv, M. Chashnikova, M. Klinkmüller, O. Fedosenko, S. Machulik, A. Aleksandrova, G. Monastyrskyi, Y. Flores, and W. T. Masselink, *Appl. Opt.* **51**, 6789 (2012).
4. R.E. Peale, E. Smith, H. Abouelkhair, I.O. Oladeji, S. Vangala, T. Cooper, G. Grzybowski, F. Khalilzadeh-Rezaie, and J.W. Cleary, *Opt. Eng.* **56**, 037109 (2017).
5. J. Nath, S. Modak, I. Rezadad, D. Panjwani, F. Rezaie, J. W. Cleary, and R.E. Peale, *Optics Express* **23**, 20366 (2015).
6. F.K. Rezaie, C.J. Fredericksen, W.R. Buchwald, J.W. Cleary, E.M. Smith, I. Rezadad, J. Nath, P. Figueiredo, M. Shahzad , J. Boroumand, M. Yesiltas, G. Medhi, A. Davis, and R.E. Peale, *MRS Online Proceedings Library Archive* 1510 (2013).
7. H. Tang, H. Berger, P.E. Schmid, and F. Levy, *Solid State Commun*. **92**, 267 (1994).
8. J.I.P., *Optical Processes in Semiconductors* (Dover, New York, 1971), p. 34-42.
9. T.S. Moss, *Optical Properties of Semiconductors* (Butterworth Scientific, London, 1959), p. 34-38.
10. H. Tang, K. Prasad, R. Sanjines, P.E. Schmid, and F. Levy, *J. Appl. Phys*. **75**, 2042 (1994).
11. H. Takikawa, T. Matsui, T. Sakakibara, A. Bendavid, and P.J. Martin, *Thin Solid Films* **348**, 145 (1999).
12. G.K. Boschloo, A. Goossens, and J. Schoonman, *J. Electrochem. Soc*. **144**, 1311 (1997).
13. A. Aoki and G. Nogami, *J. Electrochem. Soc.* **143**, L191 (1996).
14. Z. Wang, U. Helmersson, and P-O. Käll, *Thin Solid Films* **405**, 50 (2002).
15. S.R. Calhoun, V.C. Lowry, R.T. Stack, R.N. Evans, J.R. Brescia, C.J. Fredricksen, J. Nath, R.E. Peale, E.M. Smith, J.W. Cleary, *MRS Advances*, submitted (2017).
16. R.J. Gonzalez, R. Zallen, and H. Berger, *Phys. Rev. B* **55**, 7014 (1997).
17. H. J. Hovel, J. Electrochem. Soc. 125, 983 (1978).
18. H. Somberg, Proc. 20th IEEE Photovoltaics Specialists Conference, p. 1557 (1988).
19. Aibin Huang, Jingting Zhu, Yijie Zhou, Yu Yu, Yan Liu, Songwang Yang, Shidong Ji, Lei Lei and Ping Jin, Nanotechnology 28, 1 (2017).